Electrical Treeing and Partial Discharge Behaviour in Epoxy Nanocomposites with in situ Synthesized SiO_2

Mohammed Mostafa Adnan, Torbjørn Andersen Ve, Sverre Hvidsten, Marit-Helen Glomm Ese, Julia Glaum, and Mari-Ann Einarsrud

***Abstract*—The electrical treeing resistance of epoxy-SiO_2 nanocomposites prepared by synthesizing functionalized SiO_2 nanoparticles directly in epoxy was investigated and compared to pure epoxy (diglycidyl ether of bisphenol-A). Partial discharge measurements indicate a transition of initially non-conducting trees to conducting trees in both the pure epoxy and the nanocomposites. A correlation between the synthesis precursors and the partial discharge behaviour over time indicates that the presence of ions and remnant precursors hasten the transition to conducting trees and lower the voltage of tree inception. The resistance to tree growth was found to be dependent on the synthesis conditions of the nanocomposites. Slower tree growth was observed in nanocomposites prepared under neutral conditions, with a homogenous dispersion of SiO_2 nanoparticles (30-50 nm, 5 wt%). The presence of ions from alkaline conditions and/or poor dispersion of SiO_2 resulted in faster and more linear tree growth and lower initiation voltages than for pure epoxy.**

***Index Terms*—epoxy, nanocomposite, partial discharge, electrical treeing, *in situ* synthesis**

I. Introduction

EPOXY nanocomposites, which typically consist of inorganic nanoparticle fillers (*e.g.*, SiO_2, TiO_2, Al_2O_3, BN, ZnO, SiC) have shown promise as nanodielectrics and as high voltage insulation materials due to improvements in their dielectric, mechanical, and thermal properties compared to pure epoxy or microcomposites [1]–[4]. The state of dispersion of the nanoparticle fillers has been demonstrated to be critical to the resulting dielectric properties of epoxy [5]–[7], including the electrical treeing resistance. Electrical treeing is one of the important precursors to dielectric breakdown in high voltage insulation. Electrical trees are dendritic gaseous channels that form from erosion of the insulation material via partial discharges (PD), initiating at locations with high electrical stress [8]–[10]. The growth of the tree, through the propagation of the channels, will eventually lead to failure in the insulating material when the tree channels reach the ground (or opposite) electrode, or reduce the dielectric strength of the material.

Various works have investigated how the treeing properties and the partial discharge behaviour of epoxy is affected by the inclusion of inorganic nanoparticles as filler. Alapati and Thomas [8] and Tanaka et al. [11] reported increased tree initiation times and slower tree growth upon inclusion of Al_2O_3 nanoparticles. Nyamupangedengu and Cornish [12] demonstrated a lower magnitude of PD in epoxy nanocomposites containing either MgO, SiO_2 or Al_2O_3, as well as distinct phase-resolved patterns of PD. Nakamura et al. [13] also reported specific phase-resolved PD patterns at different stages of tree growth, as well as a transition from branched to bushy trees with increasing nanoparticle (SiO_2) content and temperature.

However, the quality of dispersion of the nanoparticles can significantly affect the resistance to tree growth in epoxy nanocomposites. Chen et al. [14] showed decreased initiation times for trees in epoxy-SiO_2 microcomposites, compared to increased initiation times in nanocomposites with layered-silicates, indicating the importance of filler particle size. Surface functionalization of SiO_2 nanoparticles with silane coupling agents (SCA) were also demonstrated to affect the dispersion of the particles significantly, which in turn improved the treeing properties [7] – the tree growth was slower and the time to failure was increased when the nanoparticles were functionalized prior to incorporation into the epoxy.

The state of dispersion of the nanoparticles is known to be affected strongly by the methods and procedures used in the preparation of the nanocomposites [5]. To the best of our knowledge, all the work investigating electrical treeing in epoxy nanocomposites employ an *ex situ* approach in the synthesis of the nanocomposite samples, where the inorganic

Manuscript received on xx Month 20yy, in final form xx Month20yy, accepted xx Month 20yy. Corresponding author: M.-A. Einarsrud.

This work is funded by the Research Council of Norway through the project "Stipendiatstillinger til SINTEF Energi AS" (Project no. 259866).

M. M. Adnan was with the Department of Materials Science and Engineering at NTNU Norwegian University of Science and Technology, Trondheim, Norway. He is now with Yara International ASA, 3936 Porsgrunn (mohammed.mostafa.adnan@yara.com)

J. Glaum, and M.-A. Einarsrud are with the Department of Materials Science and Engineering at NTNU Norwegian University of Science and Technology, Trondheim, Norway (e-mail: julia.glaum@ntnu.no, mari-ann.einarsrud@ntnu.no).

T. A. Ve, S. Hvidsten, and M.-H. G. Ese are with SINTEF Energy AS, Trondheim, Norway (email: torbjornandersen.ve@sintef.no, sverre.hvidsten@sintef.no, marit-helen.ese@sintef.no).

Color versions of one or more of the figures in this article are available online at http://ieeexplore.ieee.org

nanoparticles are pre-synthesized and physically mixed with the epoxy resin. Dispersion of the nanoparticles in the viscous epoxy in such an approach is difficult, and it can be challenging to consistently ensure a satisfactory state of dispersion with minimal agglomeration. An alternative approach is to synthesize the nanoparticles directly in the epoxy resin by the reaction of precursor materials. Several works have used the sol-gel method to prepare epoxy-SiO_2 nanocomposites via the hydrolysis and condensation of alkoxide precursors in epoxy [15]–[21]. The parameters for *in situ* syntheses of inorganic nanoparticles (e.g., precursors, pH, surface functionalization, catalysts) can also be controlled to alter the morphology and state of dispersion of the nanoparticles [22]. Several works have demonstrated how the dispersion of nanoparticles improves considerably when using an *in situ* approach compared to an *ex situ* one [23]–[25]. However, there are no investigations of the electrical treeing properties of epoxy nanocomposites prepared using such *in situ* techniques.

The use of an aqueous sol-gel method for the preparation of epoxy nanocomposites with inorganic oxide fillers is therefore a novel approach in the field of nanodielectrics. The aim of this work is to study how the tree initiation, the tree growth and morphology, and the partial discharge behaviour in epoxy-SiO_2 nanocomposites are affected when this method is used instead of a traditional preparation process involving physical mixing of nanoparticles. The main application for the epoxy nanocomposites in this work was for the impregnation of hydrogenator stator bars, which are initially insulated using mica tape prior to impregnation. Pure epoxy is used as a reference for comparison with the nanocomposites. The effects of the state of dispersion of the nanoparticles, which was changed by adjusting the pH and amount of coupling agent used, is discussed.

II. Experimental

A. Preparation of samples

Samples for electrical treeing were prepared with a needle-plane geometry, using stainless steel acupuncture needles from Hegu Svenska AB, with 5 µm tip radius, 0.3 mm diameter, and a needle-plane gap of 2 mm ± 0.3 mm. Brass bars were used as the plane (ground) electrode. An example of a sample (pure epoxy) after curing is shown in Figure 1a. The embedding of the ground electrode and high voltage needle was checked using an optical microscope – any samples exhibiting a loss of adhesion or debonding at the interfaces were discarded.

Diglycidyl ether of bisphenol-A (DGEBA) was used as the epoxy resin, along with the curing agent poly(propylene glycol) bis(2-aminopropyl ether). Pure epoxy samples were prepared by mixing the resin with the curing agent in a PET beaker at room temperature and under vacuum. The mixture was then poured into moulds for the treeing samples, and then cured at 100 °C for 5 h in 10 bar N_2. The N_2 pressurization was used to remove micro-voids in the samples, and the pressure was released slowly after curing was complete.

The nanocomposites (all with 5 wt% SiO_2) were prepared using the *in situ* procedure described in [6]. DGEBA was heated to 80 °C in a round-bottom flask with a reflux condenser. 3-(aminopropyl) triethoxysilane (APTES) was added as an SCA and mixed for 1 h. The temperature was reduced to 60 °C and tetraethyl orthosilicate (TEOS) was mixed for 1 h as the SiO_2 precursor. Distilled water was then added, and the reaction mixture was stirred for 4 h, before increasing the temperature to 80 °C for another 1 h. The pH of the water was adjusted to 7 or 11 using ammonia solution (35 wt%). The mixture was then poured into a PET beaker and stirred overnight (15-18 h) at 80 °C. The curing agent was then added and mixed under vacuum at room temperature before the mixture was poured into the moulds and cured using the same conditions as for pure epoxy. Two different sets of *in situ* nanocomposites were prepared: samples prepared with an APTES:DGEBA ratio of 1:10 are referred to as EAS10, and samples prepared with an APTES:DGEBA ratio of 1:30 are referred to as EAS30. All the EAS10 samples were prepared at pH 7, while the EAS30 samples were prepared at bot pH 7 and pH 11.

B. Electrical treeing procedure

Figures 1b and 1c show a picture and a schematic, respectively, of the experimental setup used for the treeing experiment. The sample was immersed in synthetic ester fluid Midel 7131 to prevent surface flashovers. The images of the tree during the experiment were captured using a camera (Photometrics Cascade II 1024 EMCCD).

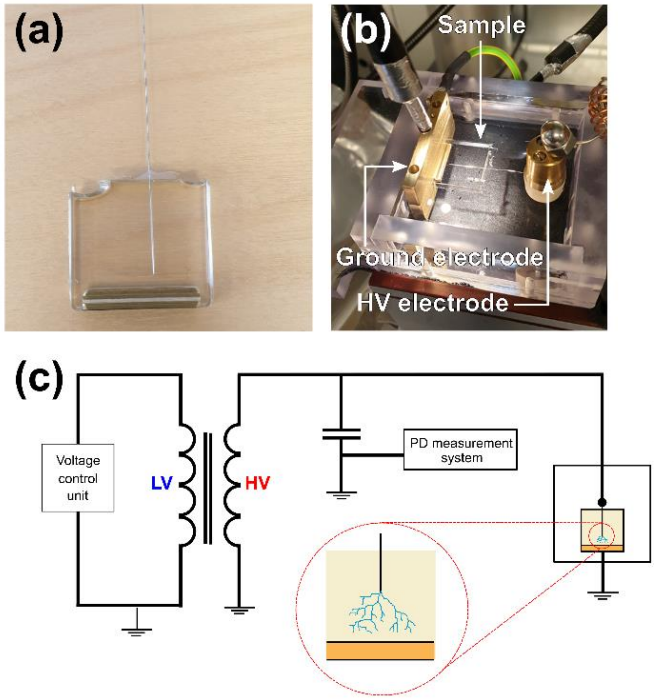

Fig. 1. (a) Pure epoxy sample after casting and curing. (b) Cell containing sample immersed in Midel 7131 and the needle connected to the high voltage (HV) electrode. (c) Schematic of circuit used for treeing experiment, showing the HV transformer, coupling capacitor, PD measurement system, and test object.

Partial discharge (PD) measurements were performed using an Omicron MPD 600 digital detector, with a threshold at 500 fC for PD measurement. A stepwise voltage ramp was used, starting at 5 kV. If a significant amount of PD was observed at the start of the measurement at 5 kV, the sample was checked again for debonding or loss of adhesion for the electrodes. Steps of 5 min duration and 2.5 kV step height were used up to 25 kV, until a tree was initiated. The initiation of the tree was defined as the formation of a single channel exceeding 30 μm. If a tree was not initiated during the increase to 25 kV, the sample was kept at 25 kV for 30 min. If tree initiation was still unsuccessful, the sample was grounded and then after at least 30 min, the procedure was repeated using larger voltage steps (5 kV). If still unsuccessful, the sample was grounded a final time before the voltage was set directly to 20-25 kV for another 30 min. If there still was no tree initiated, the sample was not tested further. When a tree was initiated, the sample was grounded, and then the voltage was set to 10 kV to investigate the tree growth.

C. Nanoparticle and tree morphology characterization

Transmission electron microscopy (TEM) images of the nanocomposites were taken using a JEOL JEM 2100F instrument at 200 kV accelerating voltage to characterize the *in situ* synthesized nanoparticles. Post-experiment optical images of the electrical trees were recorded using a Keyence Digital Microscope and were used to measure the tree channel widths and the horizontal tree spread. An average channel width was obtained using ten randomly selected points on the trees. Image processing was performed on the software ImageJ 1.51j8. Fractal dimension analysis was performed by employing the box-counting method, using binary images of the trees obtained via thresholding of the camera images.

III. Results

A. Nanocomposite morphology

Figure 2 shows the morphology and state of dispersion of the *in situ* synthesized SiO_2 in the EAS10 (Figure 2a) and EAS30 (Figure 2b) samples. At pH 7 and with increased surface functionalization, the SiO_2 clusters were 30-50 nm with a free space length (L_f) of ~80 nm, whereas at pH 11 and with less APTES for surface functionalization, the SiO_2 nanoparticles form larger clusters (90-120 nm) with larger regions of unfilled polymer (L_f of 200-225 nm).

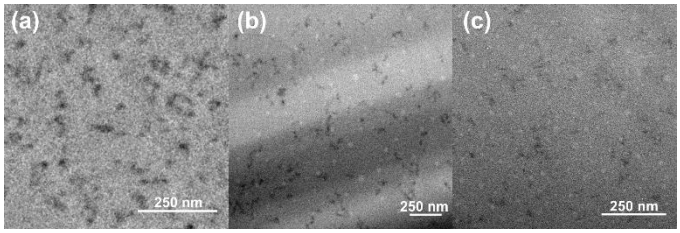

Fig. 2. Representative TEM images of epoxy-SiO_2 nanocomposites (5 wt%) prepared with the *in situ* process with (a) pH 7 and 1:10 ratio of APTES:DGEBA (EAS10), (b) pH 11 and 1:30 ratio of APTES:DGEBA (EAS30 pH 11), and (c) pH 7 and 1:30 ratio of APTES:DGEBA (EAS30 pH 7).

Other physical and chemical properties of the nanocomposites (reaction mechanism, glass transition, dielectric and infrared spectroscopy) were studied and described in a previous publication [6].

B. Tree initiation voltage and time

All the samples, whether pure epoxy or nanocomposite, exhibited a resistance to tree initiation even at 25 kV. Of the 10 samples prepared for each composition, trees were initiated in only 4 samples from each composition. Table 1 shows the initiation voltages and time held at that voltage for the samples where a tree was initiated. The pure epoxy appears to be more resistant to tree initiation, as a higher voltage and generally longer time was required to initiate the trees compared to the nanocomposites. Additionally, after grounding and setting the voltage to 10 kV for the growth period, the pure epoxy samples did not exhibit any growth for 20-30 min, whereas the trees in most of the nanocomposite samples all began to grow immediately. The nanocomposite samples prepared at pH 7 usually exhibit similar initiation voltages as pure epoxy (~20 kV), whereas some of the samples prepared at pH 11 exhibit a slightly lower initiation voltage (10-15 kV). No direct correlation could be observed in the tree initiation times for the different samples.

TABLE I
VOLTAGE AND TIME REQUIRED FOR TREE INITIATION.

Sample composition	Sample no.	Initiation voltage [kV]	Initiation time at voltage [s]
Pure epoxy	1	25	60
	2	25	- [a]
	3	25	1573
	4	25	800
EAS10	1	20	721
	2	20	501
	3	10	110
	4	20	104
EAS30 (pH 11)	1	10	190
	2	10	0
	3	15	104
	4	20	370
EAS30 (pH 7)	1	25	117
	2	20	37
	3	25	374
	4	20	84

[a] Data not available.

C. Tree growth and shape

The presence of SiO_2 nanoparticles was observed to affect both the shape and speed of growth of the electrical trees. Figure 3 shows selected samples of pure epoxy, and nanocomposites with compositions EAS10 (pH 7) and EAS30 (both pH 7 and 11). The trees in pure epoxy grew more homogeneously, with branches forming and developing evenly, whereas in the nanocomposites there are fewer branches that grow to an extensive length, and the growth is not even in all the branches, resulting in smaller “buds” or “pine-cone” structures in certain regions. Figure 4 displays the growth of the trees over time, where it is observed that the nanocomposites prepared with a larger amount of APTES (EAS10) exhibit a slower tree growth than pure epoxy. However, there is a noticeable difference between the EAS30 samples prepared at pH 7 and at pH 11,

with those at pH 11 showing a much faster growth rate from the start. The EAS30 pH 7 samples exhibit a slightly faster growth rate than pure epoxy after the initial period (~20 min). The overall growth rates (measured as the final vertical tree length divided by the total time taken), the horizontal spread (maximum horizontal distance between two points of the tree), the average channel widths, and the fractal dimensions (D_f) of the trees are listed in Table 2. The average horizontal spread of the trees is slightly lower in the nanocomposites prepared at pH 7, compared to pure epoxy, but it is significantly narrower in the EAS30 nanocomposites prepared at pH 11. Additionally, the average channel width of the fine tree branches in the EAS30 nanocomposites is also noticeably smaller in most of the samples, whereas for the EAS10 nanocomposites there is no significant change from those observed in pure epoxy.

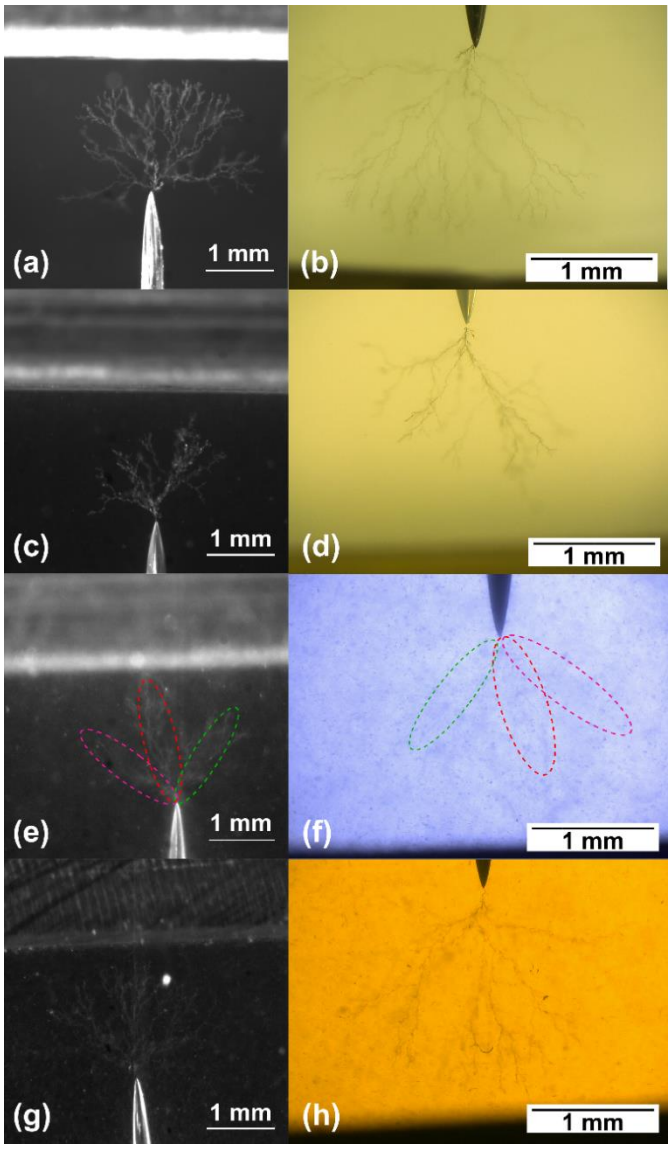

Fig. 3. Camera (left) and optical microscope (right) images of electrical trees from selected samples: (a, b) Pure epoxy; (c, d) EAS10 nanocomposite; (e, f) EAS30 (pH 11) nanocomposite; (g,h) EAS30 (pH 7) nanocomposite.

The tree morphologies were also characterized using the fractal dimension (D_f), where $1 < D_f < 2$ represents branched trees and $2 < D_f < 3$ represents bushy trees. Figure 5 shows a comparison of the trees and their binary representations from which the fractal dimensions were calculated. The EAS10 nanocomposites generally exhibit a smaller D_f than pure epoxy, whereas EAS30 nanocomposites at pH 7 exhibited a higher fractal dimension, close to 2. The D_f for EAS30 nanocomposites prepared at pH 11 could not be measured due to the poor contrast difference between the trees and the epoxy in the images, which prevented accurate thresholding to form the binary images required for the analysis.

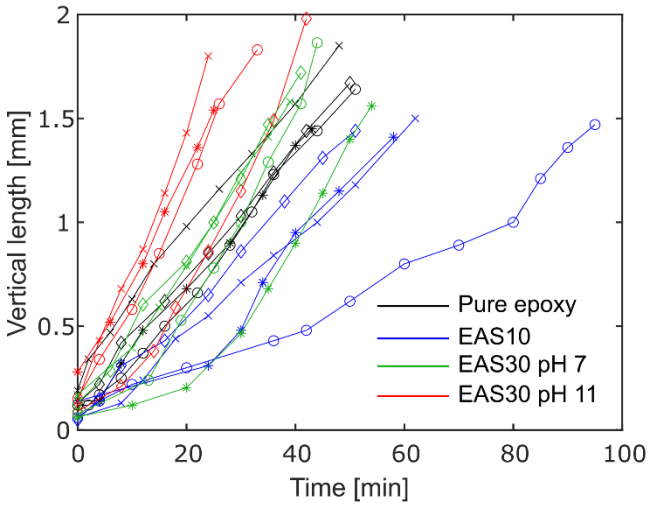

Fig. 4. Electrical tree growth progress showing the increase in vertical length (directly from the needle towards the ground electrode) over time (measured from start of growth) at 10 kV.

TABLE II

AVERAGE PROPERTIES OF THE ELECTRICAL TREES IN PURE EPOXY AND DIFFERENT TYPES OF EPOXY-SiO_2 NANO-COMPOSITES

Sample	Growth rate [mm min^{-1}]	Spread [mm]	Average channel width [μm]	D_f [1]
Pure epoxy (1)	0.030	2.5	4.2	1.47
Pure epoxy (2)	0.035	2.9	4.6	1.47
Pure epoxy (3)	0.030	2.3	2.4	1.48
Pure epoxy (4)	0.031	3.1	4.0	1.91
EAS10 (1)	0.015	1.9	4.8	1.47
EAS10 (2)	0.023	2.3	4.3	1.26
EAS10 (3)	0.022	2.1	3.9	1.37
EAS10 (4)	0.028	2.7	3.7	1.89
EAS30 pH 11 (1)	0.051	1.0	3.6 [2]	-
EAS30 pH 11 (2)	0.069	1.5	2.9	-
EAS30 pH 11 (3)	0.050	1.6	1.9	-
EAS30 pH 11 (4)	0.045	1.7	1.9	-
EAS30 pH 7 (1)	0.041	2.6	2.1	-
EAS30 pH 7 (2)	0.036	2.0	2.2	1.89
EAS30 pH 7 (3)	0.039	2.7	1.7	1.91
EAS30 pH 7 (4)	0.030	1.9	2.2	1.91

[1] The fractal dimensions could not be obtained for some of the EAS30 samples.

[2] The average fine tree channel width is reported here, although this sample exhibited a very bushy region at the needle tip with channels of up to 20 μm.

As seen in Figure 5, the trees are much narrower as well in all the EAS30 nanocomposites, with most of the branches grouped closer together. In comparison, all the electrical trees in the pure epoxy were more uniform, with the tree branches growing more homogeneously in a "broccoli-head" shape. The trees in the EAS10 nanocomposite samples exhibited morphologies similar to those in pure epoxy, but with a narrower spread of the tree branches and slightly closer packed branches.

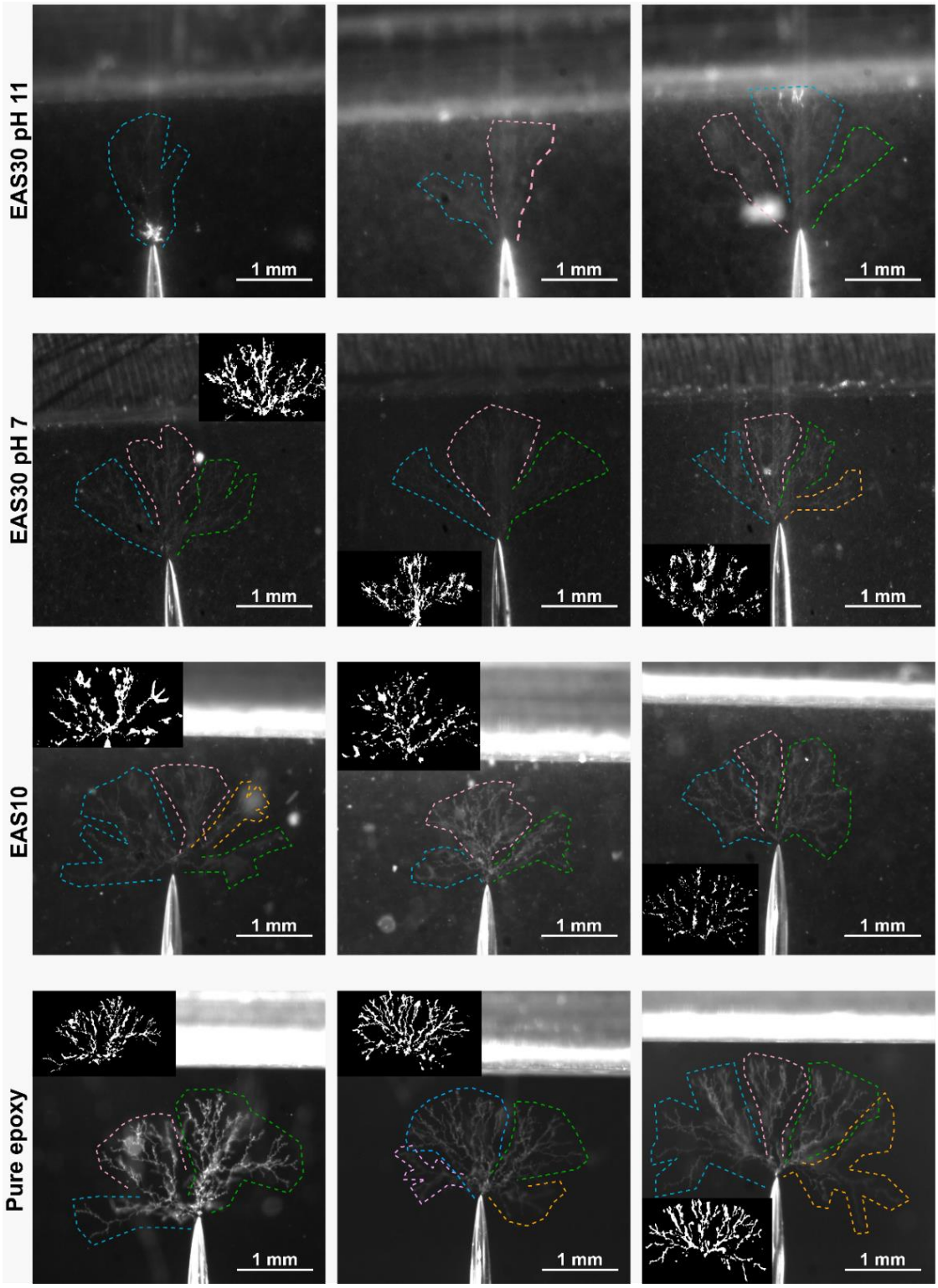

Fig. 5. Illustration of the different groups of branches (indicated by different colored dashed lines) in the electrical trees formed in (from bottom to top): pure epoxy, EAS10 nanocomposites, EAS30 nanocomposites at pH 7, and EAS30 nanocomposites at pH 11. The insets alongside the camera images show the binary representations of the trees used to calculate D_f. The branch groupings were determined from optical microscope images.

D. Phase-resolved partial discharge patterns

Both the pure epoxy and the nanocomposites exhibit similar phase-resolved partial discharge (PRPD) patterns at different phases of treeing. Right after initiation of electrical trees, the PD activity was high and typically formed two distinct regions, as shown in Figure 6a. The first region consists of a triangular shape with a higher average discharge magnitude and is referred to as "wing-like" PD. The second region generally has lower discharge magnitude with a more symmetrical and flatter shape, and is referred to as "turtle-like" PD [9]. Both these types of PD resemble what is commonly called "rabbit ear" PDs, which correspond to discharges in voids. These PRPD patterns persist in the first stage of the treeing process when the tree is still close (up to 200 µm) to the high voltage needle. As the tree extends further away from the needle, and fewer "new" branches are formed close to the needle, both the PD discharge and activity level become significantly lower, only forming scattered patterns resembling turtle-like regions, as highlighted in Figure 6b. The magnitude of the turtle-like PD in the later stages of treeing did not exceed 0.010 nC in the pure epoxy, while in EAS10 and EAS30 the PD activity in later stages of treeing (generally after 20 min) was minimal with very low discharge magnitude (below 0.005 nC).

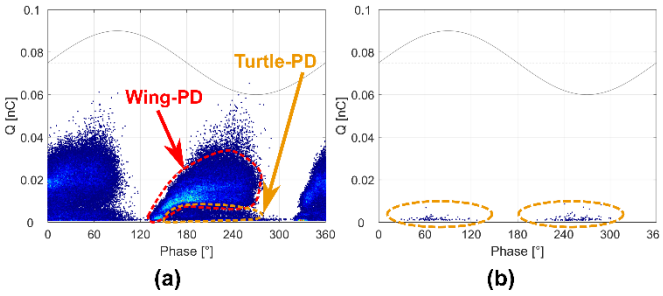

Fig. 6. Phase-resolved partial discharge (PRPD) patterns (a) during the first stage of treeing right after initiation, and (b) during the later stages of fine tree growth. The red and orange regions designate the wing-like and turtle-like PD patterns, respectively.

However, some exceptions have been observed during the initial treeing stage in some nanocomposites, where multiple wing-like PD regions formed. An example is demonstrated in Figure 7, where the PD patterns over different time periods after the tree initiation are shown alongside images of the tree at the end of each time period. This is the same EAS10 sample that exhibited the slowest growth (labelled as -o- in blue in Figure 4). Such extensive PD activity with multiple wing-like and turtle-like PD was only observed in the nanocomposites, in periods when the growth of the tree was slowest. In some periods, as shown in Figure 7c, certain regions in the PD pattern were disconnected (floating) and appeared to be a combination of wing and turtle-like PD.

Although Figure 7 shows extensive wing-like PD activity up to 38 min after tree initiation, it should be noted that this was an exception rather than the rule. Generally, the wing-like PD activity ceased in most samples between 3 and 20 min, before the activity decreased and only scattered turtle-like PD activity was registered for the remainder of the treeing process.

IV. Discussion

A. Effect of the synthesis conditions on the electrical treeing properties

The initiation of trees is a stochastic process that is dependent on not only the strength of the electrical field, but also the presence of defects or sources of electrons near the needle tip for sufficiently high discharges that can erode through the material. One possible reason for the low tree initiation rate (~ 40 %) is the use of N_2 pressurization during the curing process, in addition to vacuum degassing during both the mixing with the curing agent and the casting. While most works in literature stress the need for vacuum before casting to remove air bubbles, which can be a severe weakness for dielectric properties, none have reported the use of a pressurized environment during casting. The higher pressure will minimize the size of any bubbles that do remain, thus further reducing the chances of any bubbles near the high voltage electrode from acting as sources of PD.

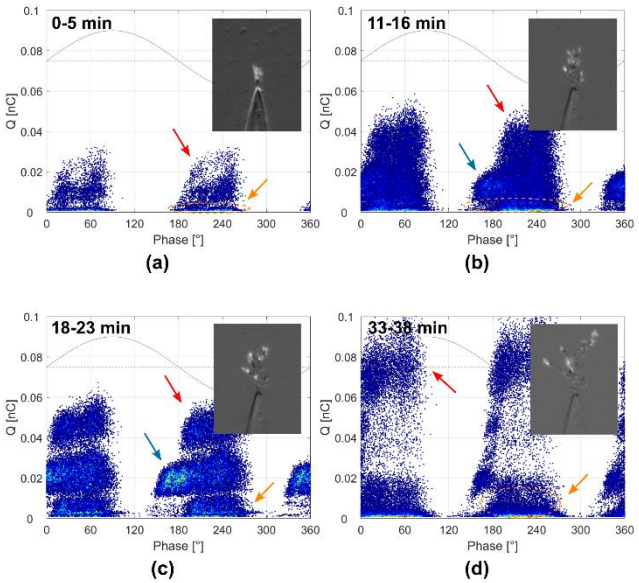

Fig. 7. Evolution of PRPD patterns in selected EAS10 nanocomposite (5 wt% SiO_2) at different time periods after tree initiation: (a) 0-5 min; (b) 11-16 min; (c) 18-23 min; (d) 33-38 min. The tree growth in these periods is shown as the bright parts in the accompanying grayscale camera images. The wing and turtle like PD regions are marked by the red and orange arrows, respectively. The blue arrows indicate PD patterns that appear to be a combination of wing and turtle-like PD.

However, in the samples where trees were successfully initiated, it appears that the pure epoxy samples generally required higher voltages for tree initiation (25 kV). Meanwhile, the nanocomposites exhibited a slightly lower initiation voltage, depending on the conditions used in the synthesis (Table 2). The general decrease in the initiation voltage in the nanocomposites observed here may be attributed to the presence of *in situ* precursors (e.g., TEOS, APTES, or water) that remain unreacted in the resin mixture, or the presence of by-products of the hydrolysis and condensation reactions that were not removed completely (e.g., ethanol). As these are liquids, they may contribute to space charges and subsequent local field enhancements. Additionally, NH_3 was used to obtain

a higher pH in the water used for the hydrolysis of TEOS in the EAS30 nanocomposites – the introduction of NH_4^+ and OH^- ions may also be a contributing factor to the lower initiation voltages in EAS30. Another possible factor could be the polarization of the nanoparticles themselves, as this would cause enhancement of the electric field near the high voltage needle, resulting in a lower apparent initiation voltage. In such a case the true initiation voltage would be difficult to determine.

The pH and amount of the silane coupling agent (APTES) used during synthesis was found to be critical in improving the quality of dispersion of the SiO_2 in the nanocomposites, as evidenced in Figure 2. A higher pH promotes faster condensation of the alkoxide precursor, and this generally results in larger and more compact SiO_2 clusters, as seen in Figure 2b compared to the clusters in Figure 2a. Additionally, the APTES acts as an anchor to the DGEBA chains for the SiO_2 that forms. With a reduction in the amount of APTES, there are fewer sites for the SiO_2 clusters forming from TEOS to attach to, and therefore there is an increase in the free space length (L_f) as the SiO_2 attaches to DGEBA chains further apart from one another. Despite the lack of large agglomerates (over 300 nm) in the recorded TEM images, the EAS30 samples were less transparent, and the camera images were of poorer quality, indicating that a certain degree of agglomeration must be present. As seen in Figure 4 and Table 2, the state of dispersion can significantly influence the resistance to electrical tree propagation.

The characteristic branching morphologies, shown in Figure 5, are corroborated by the calculated fractal dimensions (D_f) for the EAS10 and pure epoxy trees. All the pure epoxy and nanocomposite samples exhibit D_f below 2, indicating branched trees. However, the slightly lower D_f in some of the EAS10 nanocomposites indicates that the degree of branching is lower. On the other hand, the EAS30 (pH 7) nanocomposites all exhibited a D_f closer to 2, indicating that the trees can be considered to be "more bushy". This distinction is seen most clearly in Figure 5 where the individual branch groups (highlighted by different colours) are narrower in the EAS30 nanocomposites than in pure epoxy – in other words, the branches tend to grow closer together, resulting in what is interpreted as a "bushier" tree.

It should be noted that despite the better dispersion of the SiO_2 nanoparticles in the EAS10 nanocomposites and the slower growth of the trees, the composites still exhibit slightly narrower trees with a lower degree of branching than the pure epoxy. This is the opposite of what has been reported previously in literature investigating treeing in SiO_2 nanocomposites, where the nanocomposites exhibited more branched trees (and in some cases of higher filler contents or temperature, quite bushy trees) [7], [13], [26]. It should be noted however that the trees in pure epoxy in the cited literature also have a significantly more linear morphology than the trees observed here. Generally, increased branching is taken as an indication of increased resistance to tree growth, as the branches form when partial discharges cannot contribute to the growth of the present channel, and instead begins the formation of a new channel through a weaker region of material. In the pure epoxy samples prepared in this work, it is possible that the use of pressurization during curing has reduced the remaining air bubbles, contributing to the increased treeing resistance.

From the optical microscope images shown in Figure 8, it is seen that in the EAS10 nanocomposites the tree branches also show a pinecone structure, where multiple small "twigs" form on the branches that do not extend further or develop into an individual branch. This morphology of the trees may be attributed to the nanoparticles impeding the growth of the twigs beyond a certain distance from the main branch, which follows the path of least resistance through the resin. So in addition to slowing the growth rate of the trees, the presence of the particles appears to limit the spread of the trees as well.

The pinecone structure is also present (but less prevalent) in the EAS30 nanocomposites prepared at pH 7, but not in those prepared at pH 11 or in pure epoxy. In these latter samples any branches that do stem from a tree channel grow into a complete channel rather than a pinecone stub. The quality of dispersion of the nanoparticles therefore has a significant effect on the treeing properties of the epoxy. While the dispersion is poorer in the EAS30 nanocomposites at both pH 7 and pH 11, the particles are not agglomerated to a significantly larger degree at pH 7, unlike at pH 11, where agglomerates exceeding 200 µm were observed. In the former case (pH 7) the growth of the tree is not too dissimilar from that in pure epoxy, albeit slightly faster, as seen in Figure 4. However, in the latter case (pH 11) the greater the tree growth rate was increased significantly. In both sets of samples, however, the tree morphology was changed from those in pure epoxy and EAS10 nanocomposites – the tree channels grew more directly towards the ground electrode, and the spread of the branches was significantly narrower.

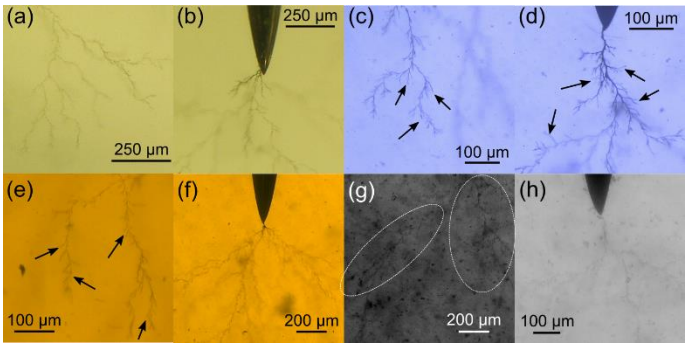

Fig. 8. Comparison of the tree branch morphologies both at the end of the tree tips and close to the needle in (a,b) pure epoxy, and in (c,d) EAS10, (e,f) EAS30 (pH 7), and (g,h) EAS30 (pH 11) nanocomposites. The arrows show pinecone-like structure in the branches. In (g) the white dotted circles indicate the areas where the tree is growing, which can be difficult to see due to poor contrast.

B. Interpreting the PD patterns during tree growth

The wing and turtle-like PD patterns observed during the tree growth (shown in Figure 6) have been reported previously in several works, although different authors suggest different sources for the PD. Wu et al. [27] and Lv et al. [9] demonstrated

similar PD patterns from trees grown in polyethylene and epoxy samples, respectively – the wing-like PD is attributed to discharges along longer tree channels (or the entire tree length) while the turtle-like PD is attributed to discharges along short tree channels or distances (e.g. at the tip of the trees). However, Dodd et al. [28] observed similar wing and turtle-like PD in non-conducting and conducting electrical trees, respectively. Champion and Dodd [29] also reported differences in the PD activity over time for branched and bushy trees. Figure 9 shows how the PD activity in the electrical trees changed over time in selected samples (when grown at 10 kV). For the pure epoxy, scattered bursts of wing-like PD were recorded during the initial period of delay where no tree growth was observed. From the point where the tree started growing, a more continuous level of wing-like PD was observed for a brief time (~3 min). For the EAS10 nanocomposites (and EAS30, but not shown here), the tree growth was immediate, and the bursts of PD were generally more frequent (shorter intervals between them). In both cases, the PD activity levelled off afterwards at a lower magnitude as only turtle-like PD was observed for the remainder of the tree growth.

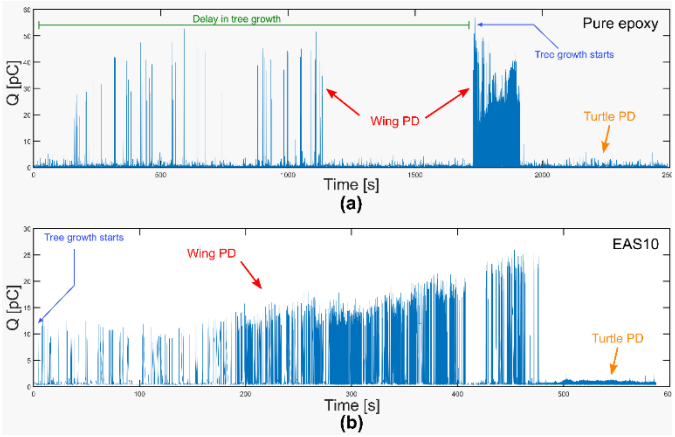

Fig. 9. PD activity over time for selected samples of (a) pure epoxy, and (b) EAS10 nanocomposite. The measurement of the PD activity was started right after tree initiation and is at 10 kV.

The initial PD behaviour is consistent with that shown by Champion and Dodd for PD in branching electrical trees [29]. However, it is unexplained as to why the wing-like PD patterns disappear as the tree grows beyond a certain distance from the needle tip. Based on the observations from Wu et al. [27] and Lv et al. [9], one can expect that with longer tree channels the wing-like patterns would still be prevalent with even larger magnitudes. A proposed explanation for this is the transition of the initiated trees from non-conducting to conducting. Figure 10a shows a schematic that describes the process as treeing proceeds. The initial tree formed at initiation is non-conducting, and the electrical field maximum lies at the tip of the high voltage needle electrode.

The build-up of potential from the needle tip to the ends of the tree causes large partial discharges in the gas-filled tree channels, which are the wing-like PD that are observed. These discharges can cause breakdown of the surrounding resin, which may result in carbonization of the channel walls, turning them conductive. As this happens, new tree channels may be initiated as well from the needle tip where the same discharge behaviour occurs. As the channels become more conductive, the front of the electrical field effectively moves away from the needle tip and closer to the ends of the tree. This means that the highest electrical field strength is no longer at the needle tip but closer to the tree tips, where the field strength is amplified due to the tree channels being narrower than the needle tip. This can also explain why tree growth can proceed at a lower voltage than the voltage required for tree initiation. Since now the distance between the electric field and the tree tips is smaller, the local electric potential is weaker as well, resulting in smaller discharges over shorter distances – in other words, the turtle-like PD. Eventually all of the tree except the tips of most branches will be conducting, and the wing-like PD is extinguished, and only turtle-like PD is observed.

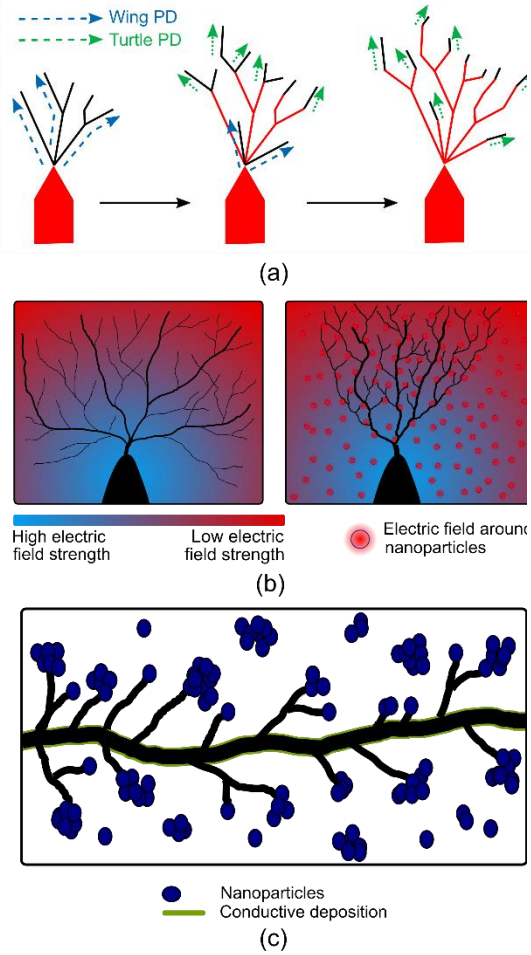

Fig. 10. (a) Schematic showing the development of the electrical tree from the needle tip (in red) along with the different types of partial discharges, and the transition from non-conducting (black lines) to conducting (red lines) tree channels. (b) The effect of the nanoparticles on the tree shape in pure epoxy (left) and nanocomposites (right), showing the change in the electric field strength. (c) How the nanoparticles prevent the growth of the tree channels, leading to the pinecone structure.

Figure 10b highlights one mechanism for how the nanoparticles can lead to the formation of a slightly narrower tree (as observed for the EAS10 samples) compared to the pure epoxy. The polarization of the particles can lead to local electric field gradients that cause the growth of the tree to be directed towards the SiO_2 particles or clusters. Figure 10c shows how this can result in the pinecone structure of the tree branches observed in Figure 8.

An additional consideration that is needed with respect to the PD activity is the presence of precursors, by-products, or ions from the *in situ* synthesis procedure. It is likely that some of these remain after the samples are casted, as previous work has indicated that the SiO_2 structures formed may not be fully condensed [6], and can potentially be another source of breakdown products in the tree channels. This would result in a faster transition to conducting tree channels in the nanocomposites and an immediate growth of the tree, thereby explaining why the trees in the nanocomposites grow at 10 kV without any delay. Additionally, such materials can also contribute to local field enhancements or accumulations of space charges, which is detrimental to the treeing resistance of the nanocomposites.

C. Further prospects for in situ materials

The use of an *in situ* synthesis approach for epoxy nanocomposites is found to be promising. As seen from the EAS10 nanocomposites, the electrical tree growth can be significantly reduced by the presence of well-dispersed SiO_2, and such a homogeneous dispersion can be achieved quite consistently using the *in situ* approach. Simultaneously, the lower degree of branching indicates the strengthening of the epoxy resin surrounding the particles, resulting in a narrower tree and limiting the spread of the damaged resin. However, the results shown in this work also highlight the importance of the selection of synthesis parameters in the preparation of nanocomposites with *in situ* synthesized nanoparticles. The lower initiation voltage for EAS10, as well as the poorer performance of the EAS30 nanocomposites (where the dispersion is poorer, but still satisfactory), shows that the presence of unreacted precursors or potential by-products must be avoided, as they can weaken regions of the epoxy resin that are unreinforced by the nanoparticles. Minimizing the presence of such defects while maintaining good control over the morphology and state of dispersion of the *in situ* synthesized nanoparticles should be emphasized for further work. The use of pressurization during curing is also recommended to minimize the air bubbles and strengthen the inherent treeing resistance of epoxy. In addition, it should be investigated how the treeing properties of these nanocomposites compare to those prepared by traditional *ex situ* approaches, and how much influence the state of dispersion exerts in them. Further experiments may also be performed by, *e.g.*, Raman spectroscopy to characterize the carbon deposit in the trees to verify whether the proposed mechanism of change in conductivity in the trees is taking place.

The *in situ* nanocomposites need not be limited to SiO_2. The selection of available alkoxide precursors for the sol-gel method means that a variety of different inorganic oxide nanoparticles can be produced [22], and further work in the preparation of nanocomposites should investigate how the type of nanoparticle may influence the electrical treeing properties.

V. Conclusions

An *in situ* sol-gel method was employed to synthesize functionalized SiO_2 nanoparticles directly in epoxy resin. The resulting nanocomposite materials, prepared using different synthesis conditions, exhibited varying resistances to electrical treeing. Nanocomposites prepared under neutral conditions (pH 7) with sufficient silane coupling agent showed a homogeneous dispersion of SiO_2 clusters (30-50 nm) and an increased resistance to electrical tree growth compared to pure epoxy (with a decrease in the average growth rate by ~27 %). On the other hand, the use of more basic conditions (pH 11) and a reduction in the amount of coupling agent resulted in a poorer state of dispersion and faster tree growth (increase in average growth rate by ~73 %). In both types of nanocomposites, the initiation voltages and the width of the trees were reduced, although this was more significant in the latter type. Partial discharge measurements indicate the formation of non-conducting trees initially, that are swiftly converted into conducting trees.

The *in situ* approach to the preparation of nanocomposites is therefore a promising avenue as it can consistently produce homogeneously dispersed nanoparticles in the epoxy, which improves the electrical treeing resistance of the material. However, care should be taken to avoid remnant materials or precursors that can cause deteriorations in the treeing resistance instead. Further work is required to establish the optimal conditions for surface modifications and dispersion, so that any potential enhancement of the electric field due to polarization of the nanoparticles can be minimized.

Acknowledgment

The authors would like to acknowledge support from the Research Council of Norway through the Norwegian Center for Transmission Electron Microscopy, NORTEM (197405/F50), and MSc Inger-Emma Nylund for taking the TEM images of the nanocomposites.

References

A. References

[1] J. K. Nelson and J. C. Fothergill, “Internal charge behaviour of nanocomposites,” *Nanotechnology*, vol. 15, no. 5, pp. 586–595, 2004, doi: 10.1088/0957-4484/15/5/032.

[2] S. Singha and M. J. Thomas, “Dielectric properties of epoxy nanocomposites,” *IEEE Trans. Dielectr. Electr. Insul.*, vol. 15, no. 1, pp. 12–23, 2008, doi: 10.1109/T-DEI.2008.4446732.

[3] M. M. Adnan *et al.*, “Epoxy-Based Nanocomposites for High-Voltage Insulation: A Review,” *Adv. Electron. Mater.*, vol. 5, no. 2, p. 1800505, 2019, doi: 10.1002/aelm.201800505.

[4] I. Plesa, P. V Notingher, S. Schlögl, C. Sumereder, and M. Muhr, “Properties of Polymer Composites Used in High-Voltage Applications,” *Polymers (Basel).*, vol. 8, no. 173, 2016, doi:

10.3390/polym8050173.

[5] C. Calebrese, L. Hui, L. S. Schadler, and J. K. Nelson, "A Review on the Importance of Nanocomposite Processing to Enhance Electrical Insulation," *IEEE Trans. Dielectr. Electr. Insul.*, vol. 18, no. 4, pp. 938–945, 2011, doi: 10.1109/TDEI.2011.5976079.

[6] M. M. Adnan *et al.*, "The Structure, Morphology, and Complex Permittivity of Epoxy Nanodielectrics with In Situ Synthesized Surface-Functionalized SiO2," *Polymers (Basel).*, vol. 13, no. 9, p. 1469, 2021, doi: 10.3390/polym13091469.

[7] S. Chen, S. Rowland, J. Carr, M. Storm, K. L. Choy, and A. J. Clancy, "The importance of particle dispersion in electrical treeing and breakdown in nano-filled epoxy resin," *Int. J. Electr. Power Energy Syst.*, vol. 129, p. 106838, Jul. 2021, doi: 10.1016/j.ijepes.2021.106838.

[8] S. Alapati and M. J. Thomas, "Influence of nano-fillers on electrical treeing in epoxy insulation," *IET Sci. Meas. Technol.*, vol. 6, no. 1, pp. 21–28, 2012, doi: 10.1049/iet-smt.2011.0046.

[9] Z. Lv, S. M. Rowland, S. Chen, H. Zheng, and I. Iddrissu, "Evolution of partial discharges during early tree propagation in epoxy resin," *IEEE Trans. Dielectr. Electr. Insul.*, vol. 24, no. 5, pp. 2995–3003, 2017, doi: 10.1109/TDEI.2017.006731.

[10] I. Iddrissu, S. M. Rowland, H. Zheng, Z. Lv, and R. Schurch, "Electrical tree growth and partial discharge in epoxy resin under combined AC and DC voltage waveforms," *IEEE Trans. Dielectr. Electr. Insul.*, vol. 25, no. 6, pp. 2183–2190, 2018, doi: 10.1109/TDEI.2018.007310.

[11] T. Tanaka, A. Matsunawa, Y. Ohki, M. Kozako, M. Kohtoh, and S. Okabe, "Treeing phenomena in epoxy/alumina nanocomposite and interpretation by a multi-core model," *IEEJ Trans. Fundam. Mater.*, vol. 126, no. 11, pp. 1128–1135, 2006, doi: 10.1541/ieejfms.126.1128.

[12] C. Nyamupangedengu and D. R. Cornish, "Time-evolution phenomena of electrical tree partial discharges in Magnesia, Silica and Alumina epoxy nanocomposites," *IEEE Trans. Dielectr. Electr. Insul.*, vol. 23, no. 1, pp. 85–94, 2016, doi: 10.1109/TDEI.2015.005055.

[13] S. Nakamura *et al.*, "Effects of temperature on electrical treeing and partial discharges in epoxy/silica nanocomposites," *IEEE Trans. Dielectr. Electr. Insul.*, vol. 27, no. 4, pp. 1169–1177, 2020, doi: 10.1109/TDEI.2020.008812.

[14] Y. Chen, T. Imai, Y. Ohki, and T. Tanaka, "Tree initiation phenomena in nanostructured epoxy composites," *IEEE Trans. Dielectr. Electr. Insul.*, vol. 17, no. 5, pp. 1509–1515, 2010, doi: 10.1109/TDEI.2010.5595552.

[15] L. Matějka, K. Dušek, J. Pleštil, J. Kříž, and F. Lednický, "Formation and structure of the epoxy-silica hybrids," *Polymer (Guildf).*, vol. 40, no. 1, pp. 171–181, 1999, doi: 10.1016/S0032-3861(98)00214-6.

[16] R. K. Donato, K. Z. Donato, H. S. Schrekker, and L. Matějka, "Tunable reinforcement of epoxy-silica nanocomposites with ionic liquids," *J. Mater. Chem.*, vol. 22, no. 19, pp. 9939–9948, 2012, doi: 10.1039/c2jm30830d.

[17] A. Afzal and H. M. Siddiqi, "A comprehensive study of the bicontinuous epoxy-silica hybrid polymers: I. Synthesis, characterization and glass transition," *Polymer (Guildf).*, vol. 52, no. 6, pp. 1345–1355, 2011, doi: 10.1016/j.polymer.2011.01.046.

[18] S. Ponyrko, L. Kobera, J. Brus, and L. Matějka, "Epoxy-silica hybrids by nonaqueous sol-gel process," *Polymer (Guildf).*, vol. 54, pp. 6271–6282, 2013, doi: 10.1016/j.polymer.2013.09.034.

[19] F. Piscitelli, M. Lavorgna, G. G. Buonocore, L. Verdolotti, J. Galy, and L. Mascia, "Plasticizing and reinforcing features of siloxane domains in amine-cured epoxy/silica hybrids," *Macromol. Mater. Eng.*, vol. 298, pp. 896–909, 2013, doi: 10.1002/mame.201200222.

[20] Y.-T. Bi, Z.-J. Li, and W. Liang, "Preparation and characterization of epoxy/\ce{SiO2} nanocomposites by cationic photopolymerization and sol–gel process," *Polym. Adv. Technol.*, vol. 25, pp. 173–178, 2013, doi: 10.1002/pat.3219.

[21] C. C. Wu and S. L. C. Hsu, "Preparation of epoxy/silica and epoxy/titania hybrid resists via a sol-gel process for nanoimprint lithography," *J. Phys. Chem. C*, vol. 114, no. 5, pp. 2179–2183, 2010, doi: 10.1021/jp908141f.

[22] M. M. Adnan, A. R. M. Dalod, M. H. Balci, J. Glaum, and M.-A. Einarsrud, "In situ synthesis of hybrid inorganic-polymer nanocomposites," *Polymers (Basel).*, vol. 10, no. 10, 2018, doi: 10.3390/polym10101129.

[23] E. Tuncer, G. Polizos, I. Sauers, D. R. James, A. R. Ellis, and K. L. More, "Epoxy nanodielectrics fabricated with in situ and ex situ techniques," *J. Exp. Nanosci.*, vol. 7, no. 3, pp. 274–281, 2012, doi: 10.1080/17458080.2010.520137.

[24] R. F. M. Elshaarawy, G. A. Seif, M. E. El-Naggar, T. B. Mostafa, and E. A. El-Sawi, "In-situ and ex-situ synthesis of poly-(imidazolium vanillyl)-grafted chitosan/silver nanobiocomposites for safe antibacterial finishing of cotton fabrics," *Eur. Polym. J.*, vol. 116, pp. 210–221, Jul. 2019, doi: 10.1016/j.eurpolymj.2019.04.013.

[25] A. R. M. Dalod, "In situ synthesis of titania and titanium based organic-inorganic nanomaterials," Norwegian University of Science and Technology (NTNU), Norway, 2017.

[26] T. Imai *et al.*, "Influence of temperature on mechanical and insulation properties of epoxy-layered silicate nanocomposite," *IEEE Trans. Dielectr. Electr. Insul.*, vol. 13, no. 1, pp. 445–452, 2006, doi: 10.1109/TDEI.2006.1624291.

[27] K. Wu, Y. Suzuoki, T. Mizutani, and H. Xie, "A novel physical model for partial discharge in narrow channels," *IEEE Trans. Dielectr. Electr. Insul.*, vol. 6, no. 2, pp. 181–190, 1999, doi: 10.1109/94.765909.

[28] S. J. Dodd, N. M. Chalashkanov, and J. C. Fothergill, "Partial discharge patterns in conducting and non-conducting electrical trees," 2010, doi: 10.1109/ICSD.2010.5568217.

[29] J. V. Champion and S. J. Dodd, "Systematic and reproducible partial discharge patterns during electrical tree growth in an epoxy resin," *J. Phys. D. Appl. Phys.*, vol. 29, no. 3, pp. 862–868, 1996, doi: 10.1088/0022-3727/29/3/053.